

Addendum to “Constraints on and future prospects for Two-Higgs-Doublet Models in light of the LHC Higgs signal”

Béranger Dumont^{1,*} John F. Gunion^{2,†} Yun Jiang^{2,‡} and Sabine Kraml^{1,§}

(1) *Laboratoire de Physique Subatomique et de Cosmologie,*

Université Grenoble-Alpes, CNRS/IN2P3,

53 Avenue des Martyrs, F-38026 Grenoble, France and

(2) *Department of Physics, University of California, Davis, CA 95616, USA*

Abstract

We update the constraints on Two-Higgs-Doublet Models of Type I and II discussed in arXiv:1405.3584 using the latest LHC measurements of the ~ 125.5 GeV Higgs signal as of Summer 2014. We provide explicit comparisons of the results before and after the Summer 2014 ATLAS and CMS updates. Overall, the changes with respect to arXiv:1405.3584 are rather small; to a large extent this is due to the fact that both the ATLAS and the CMS updates of the $\gamma\gamma$ decay mode moved closer to SM expectations.

* dumont@lpsc.in2p3.fr

† jfgunion@ucdavis.edu

‡ yunjiang@ucdavis.edu

§ sabine.kraml@lpsc.in2p3.fr

I. INTRODUCTION

In a recent paper [1], we provided a comprehensive analysis of the status of Two-Higgs-Doublet Models (2HDMs) of Type I and Type II, considering both the cases where the observed Higgs particle at the LHC is the lighter CP-even state h or the heavier CP-even state H . To this end, we performed scans of the 2HDM parameter space taking into account all relevant constraints from precision electroweak data, from stability, unitarity and perturbativity of the potential, as well as from B physics and from the direct searches at LEP. We also employed the most recent limits from searches for heavy Higgs-like states at the LHC. The central piece of the analysis however was to check for consistency with the various signal strength measurements of the observed ~ 125.5 GeV Higgs boson at the LHC, including a consistent treatment of “feed down” from the production of heavier Higgs states. This was done based on the results published by ATLAS and CMS by June 2013, *i.e.* according to the status of the Moriond and LHCP 2013 conferences (see [2] for a summary).

Since then, a number of new measurements or updates of existing ones were published by the experimental collaborations. Most significant, from the point of view of our analysis of the 2HDMs, were the long-awaited final results for the $\gamma\gamma$ decay mode from CMS [3] in July and the update of the $\gamma\gamma$ results from ATLAS [4] at the end of August 2014. There were also several other important new measurements or updates; for example uncertainties have been significantly reduced for the fermionic channels, particularly for $H \rightarrow b\bar{b}$ in $t\bar{t}H$ production. All these new results were put together and analyzed in global coupling fits in [5].

In the present note, we now revisit the analysis of [1] and ask what are the implications in the 2HDM context of all these new (or updated) results on the signal strengths of the ~ 125.5 GeV Higgs boson. To this aim, we take the scan points of [1] and, leaving everything else the same, update the χ^2 calculation for the signal strengths at 125.5 GeV in the $\mu_{\text{ggF}+t\bar{t}H}(Y)$ versus $\mu_{\text{VBF}+\text{VH}}(Y)$ planes, Eq. (5) of [1], with the new numbers presented in Table I of [5]. Points for which $\chi_Y^2 < 6.18$ for each decay mode $Y = \gamma\gamma, VV(= WW, ZZ), b\bar{b}, \tau\tau$ (that means points that are consistent within 95.4% confidence level (CL) with the observed signal strengths for each decay mode Y) and that in addition pass all other relevant constraints will be called “postLHC8(2014)-FDOK” and compared to the corresponding points of [1], called “postLHC8(2013)-FDOK”. In the plots, we will moreover identify the points

that fit both the 2013 and the 2014 analyses as “postLHC8(2013 & 2014)-FDOK”.

We note that in this addendum we focus on pointing out the small modifications that arise from the latest ATLAS and CMS results. For a detailed physics discussion and implications for future measurements, *e.g.* at the next run of the LHC at $\sqrt{s} = 13\text{--}14$ TeV, we refer to the main paper [1], whose results overall remain perfectly valid. For notations and conventions, we also refer to [1].

II. $m_h \sim 125.5$ GeV SCENARIOS

We begin by showing in Fig. 1 the points surviving all constraints in the $\cos(\beta - \alpha)$ versus $\tan\beta$ plane for the $m_h \sim 125.5$ GeV scenarios. The red points satisfy the Higgs signal constraints from both 2013 and 2014, while orange (blue) points pass only the 2014 (2013) Higgs constraints. We see that, in Type I, large values of $|\cos(\beta - \alpha)|$ get slightly more constrained, while in Type II there is a narrow strip around $\cos(\beta - \alpha) \approx -0.1$ and $\tan\beta \lesssim 2$ that is now excluded. On the other hand, in Type II slightly larger positive values of $\cos(\beta - \alpha)$ are allowed from the 2014 measurements. (Such orange points, which were not compatible with the 2013 results but are now allowed after the 2014 updates

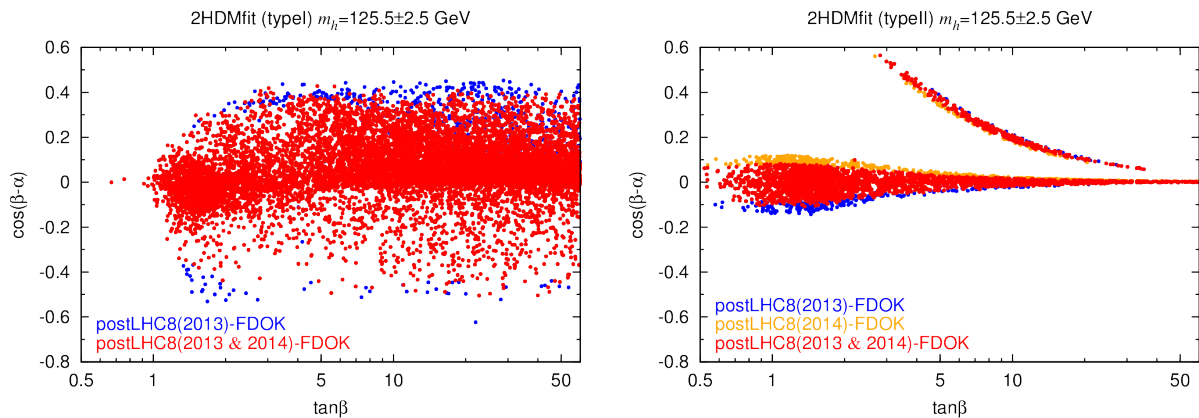


FIG. 1. Constraints in the $\cos(\beta - \alpha)$ versus $\tan\beta$ plane for $m_h \sim 125.5$ GeV. Blue points are those which passed all constraints given the Higgs signal strengths as of Spring 2013 (*i.e.* the status considered in [1]), red points are those which remain valid when employing the Summer 2014 updates, and orange points are those newly allowed after the Summer 2014 updates. Note that the latter occur only in Type II but not in Type I models.

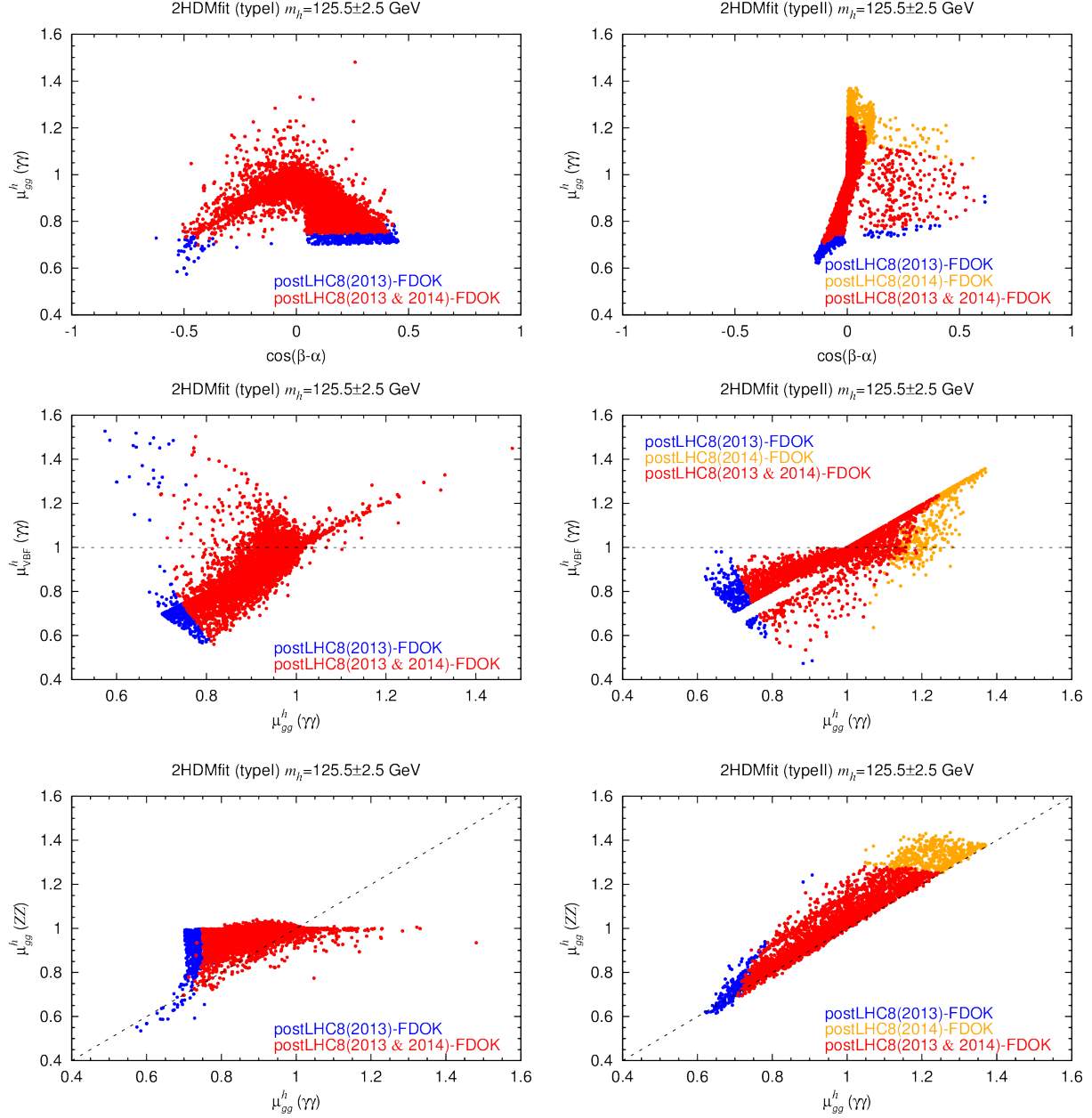


FIG. 2. As in Fig. 1, but for $\mu_{gg}^h(\gamma\gamma)$ and $\mu_{VBF}^h(\gamma\gamma)$ signal strengths versus $\cos(\beta - \alpha)$ (top row), $\mu_{VBF}^h(\gamma\gamma)$ versus $\mu_{gg}^h(\gamma\gamma)$ (middle row), and $\mu_{gg}^h(ZZ)$ versus $\mu_{gg}^h(\gamma\gamma)$ (bottom row).

do occur only in Type II but not in Type I.) The banana-shaped branch spanning from $(\tan\beta, \cos(\beta - \alpha)) \approx (3, 0.6)$ to $(40, 0.1)$ is still present; this corresponds to the solution with a flipped sign for C_D .

The reason for these slight changes lies mostly in the new combined signal strengths for the $\gamma\gamma$ decay mode: $\hat{\mu}_{ggF+ttH}(\gamma\gamma) = 1.25 \pm 0.24$ and $\hat{\mu}_{VBF+VH}(\gamma\gamma) = 1.09 \pm 0.46$ with a correlation

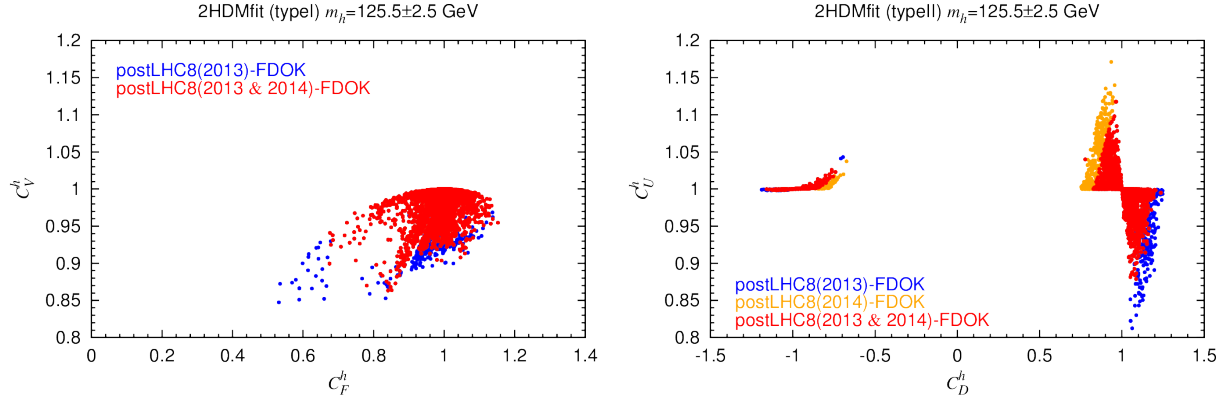


FIG. 3. Reduced couplings C_V^h vs. C_F^h in Type I (left plot) and C_U^h vs. C_D^h in Type II (right plot) for $m_h \sim 125.5$ GeV scenarios.

of $\rho = -0.30$ [5], as compared to $\hat{\mu}_{\text{ggF}+\text{ttH}}(\gamma\gamma) = 0.98 \pm 0.28$ and $\hat{\mu}_{\text{VBF}+\text{VH}}(\gamma\gamma) = 1.72 \pm 0.59$ with a correlation of $\rho = -0.38$ in 2013 [2]. The result, after combining ATLAS and CMS data, is that the best-fit signal strength in the ggF mode¹ has increased (although the new central value is consistent at the 1σ level with the 2013 results) while that in VBF+VH production has come down by a bit more than 1σ . The $\gamma\gamma$ signal strengths as a function of $\cos(\beta - \alpha)$ are shown in the top row of Fig. 2. Here, one sees explicitly that the low values of $\mu_{\text{gg}}^h(\gamma\gamma) \approx 0.6 - 0.7$ are no longer allowed. Moreover, while there has been no change in the maximum $\mu_{\text{gg}}^h(\gamma\gamma)$ obtainable in Type I, higher values up to about $\mu_{\text{gg}}^h(\gamma\gamma) \approx 1.4$ (vs. ~ 1.2 before) are attainable in Type II. The alert reader will have noticed that this upper limit is much lower than the 2σ range that should be allowed in principle. The limitation in fact comes from the $h \rightarrow VV (= WW, ZZ)$ decay mode in ggF production, for which we have $\hat{\mu}_{\text{ggF}+\text{ttH}}(VV) = 1.03 \pm 0.17$ from the 2014 measurements, and hence $\mu_{\text{gg}}^h(ZZ) < 1.37$ at 95.4% CL (as compared to $\hat{\mu}_{\text{ggF}+\text{ttH}}(VV) = 0.91 \pm 0.16$ in Spring 2013). The correlations between signal strengths in different channels are illustrated in the middle and bottom rows of Fig. 2.

In Fig. 3, we plot C_V^h vs. C_F^h (Type I) and C_U^h vs. C_D^h (Type II) for the $m_h \sim 125.5$ GeV scenarios. Substantial suppression of the fermionic couplings is possible in both models. In both cases, an enhanced $h \rightarrow \gamma\gamma$ rate can come from a suppression of C_D , which suppresses $\mathcal{B}(h \rightarrow b\bar{b})$. In Type I, since $C_U = C_D \equiv C_F$, this goes hand-in-hand with a reduction of

¹ In ttH production, uncertainties are still too large to have any impact.

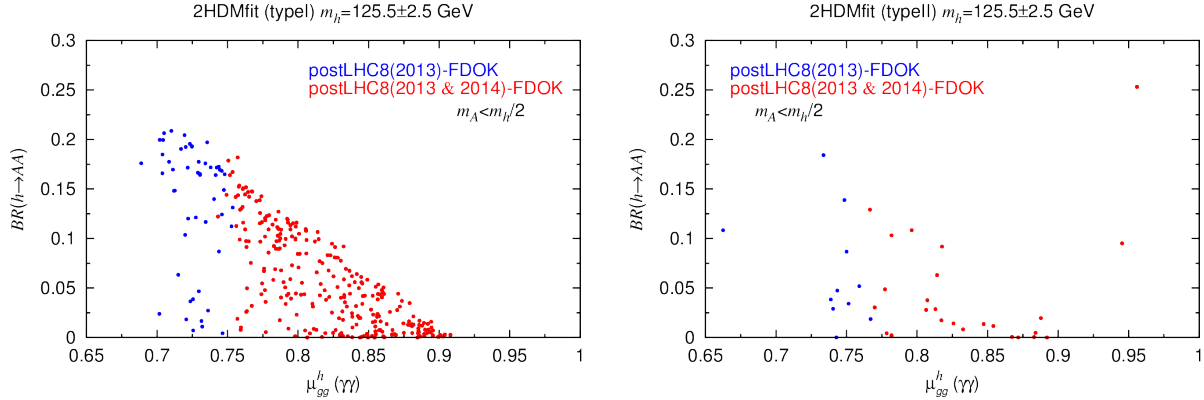


FIG. 4. Correlation of $\mathcal{B}(h \rightarrow AA)$ and $\mu_{gg}^h(\gamma\gamma)$ for $m_h \sim 125.5$ GeV scenarios with $m_A < m_h/2$.

the hgg coupling; depending on which effect dominates, $\mu_{\text{VBF}}^h(\gamma\gamma)$ can be enhanced, while $\mu_{gg}^h(\gamma\gamma)$ is suppressed (cf. the middle-left plot in Fig. 2). This does not occur in Type II, where enhancement/suppression of C_U and C_D is anti-correlated. In this case $C_D < 1$ leads to an enhancement and $C_D > 1$ to a suppression of both $\mu_{gg}^h(\gamma\gamma)$ and $\mu_{\text{VBF}}^h(\gamma\gamma)$; since C_U works in the same direction, the effect can be more pronounced for $\mu_{gg}^h(\gamma\gamma)$ than for $\mu_{\text{VBF}}^h(\gamma\gamma)$ (cf. the middle-right plot in Fig. 2)

Regarding the allowed ranges of m_H , m_A and m_{H^\pm} , there is no visible change with respect to [1]. It is however interesting to take a closer look at the region $m_A < m_h/2$, where $h \rightarrow AA$ decays are possible. In Fig. 4, we show the correlation between $\mathcal{B}(h \rightarrow AA)$ and $\mu_{gg}^h(\gamma\gamma)$. As one can see, large values of the former imply suppression of the latter. Although the effect is small, the requirement $\mu_{gg}^h(\gamma\gamma) > 0.77$ at 2σ constrains the maximum $\mathcal{B}(h \rightarrow AA)$ that can be obtained in Type I and Type II models. (In Type II, however, a focused scan would be needed for a quantitative interpretation of the results.) This limit is actually stronger than the “direct” constraint on unseen decays, $\mathcal{B}_{\text{new}} < 0.22$ [5], from the generic C_U , C_D , $C_V < 1$ coupling fit.

III. $m_H \sim 125.5$ GeV SCENARIOS

Let us now turn to the case that the observed Higgs state at ~ 125.5 GeV is the heavier CP-even scalar H . Analogous to Fig. 1, we show in Fig. 5 the $m_H \sim 125.5$ GeV points in the $\sin(\beta - \alpha)$ versus $\tan \beta$ plane after all constraints have been applied. As before, we observe a slight narrowing of the allowed $\sin(\beta - \alpha)$ range, but no visible change in the

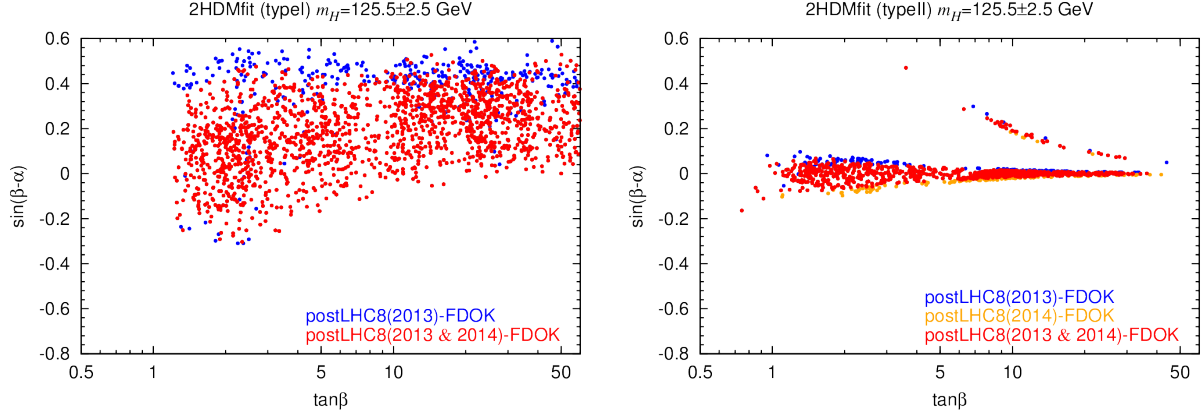


FIG. 5. Constraints in the $\sin(\beta - \alpha)$ versus $\tan \beta$ plane for $m_H \sim 125.5$ GeV, comparing the current status as of Summer 2014 to that of Spring 2013.

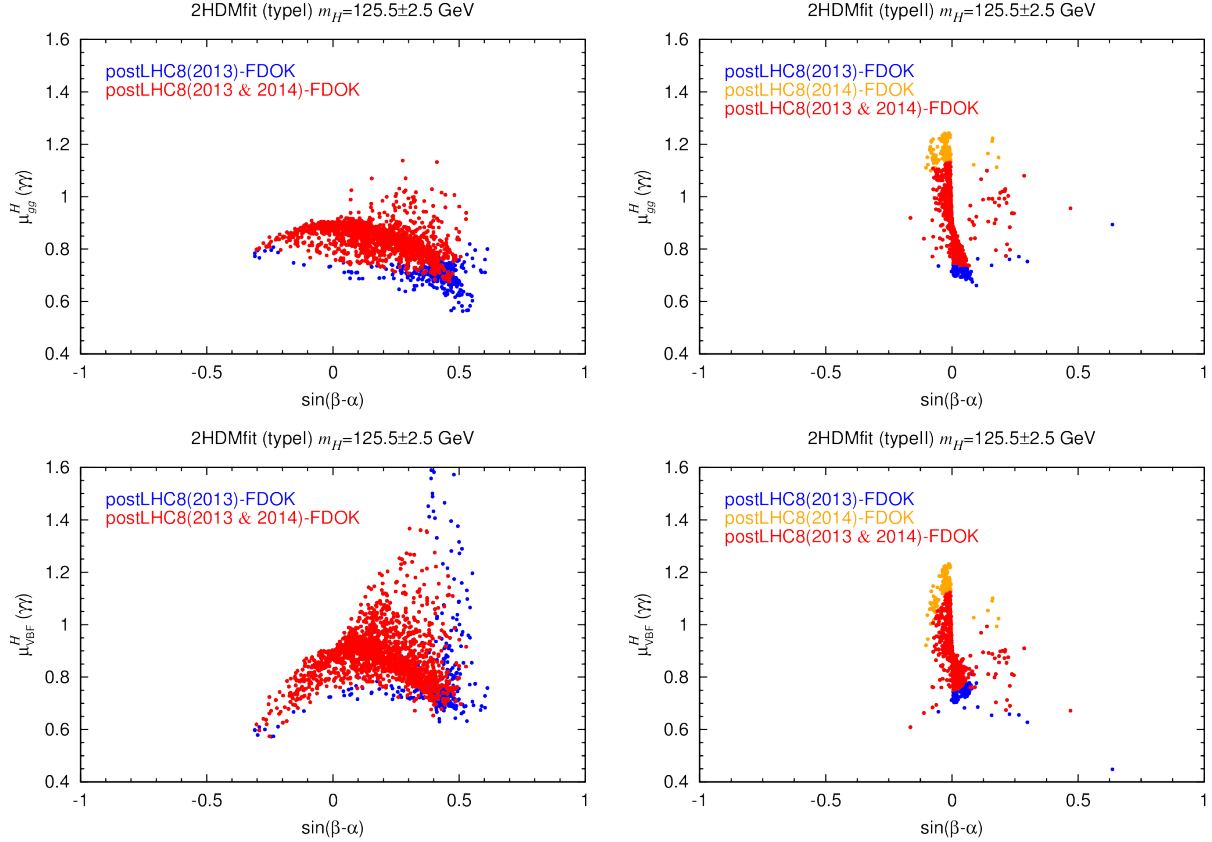


FIG. 6. As Fig. 5, but for the $\gamma\gamma$ signal strengths versus $\sin(\beta - \alpha)$.

$\tan \beta$ direction. It is interesting to note, however, that in Type I $m_H \sim 125.5$ GeV requires $\tan \beta \gtrsim 1$. It is also remarkable that, while in Type I $\sin(\beta - \alpha)$ can still vary from about -0.3 to 0.5 (corresponding to $C_V \gtrsim 0.87$), in Type II one is pretty much forced into the

decoupling/alignment regime, the few points with sizable $\sin(\beta - \alpha)$ being quite rare and associated with the branch having a negative sign for C_D^H .

The $\gamma\gamma$ signal strengths as a function of $\sin(\beta - \alpha)$ are shown in Fig. 6. Correlations of signal strengths are illustrated in Fig. 7. Analogous arguments as for the $m_h \sim 125.5$ GeV case apply. It is however worth noting that the direct correlation between $\mu_{gg}^H(\gamma\gamma)$, $\mu_{VBF}^H(\gamma\gamma)$ and $\mu_{gg}^H(ZZ)$ in Type II is much stronger than for $m_h \sim 125.5$ GeV. As above, additional Type II points occur with $\mu_{gg}^H(\gamma\gamma)$ and $\mu_{gg}^H(ZZ)$ values beyond those found in [1]. These would be removed if future measurements show that $\mu_{gg}^H(\gamma\gamma)$ ($\mu_{gg}^H(ZZ)$) is within 10% (20%) of unity. As was noted in [1], if $\leq \pm 5\%$ deviations from the SM are required for both the ZZ and $\gamma\gamma$ final states then the upper plots show that only a few points of the Type I model having $\mu_{gg}^H(\gamma\gamma) \gtrsim 0.95$ can survive and that *all* Type II points will be removed by this constraint.

As regards the h , A and even the H^\pm masses associated with a good fit by the H to the LHC data and other limits, there is not much change with respect to [1]. In particular the range of h and A masses discussed in [1] remains valid, the only modification is the slight narrowing in $\sin(\beta - \alpha)$ already visible in Fig. 5.

IV. CONCLUSIONS

Overall, the new ATLAS and CMS analyses from Summer 2014 lead to relatively minor modifications of the preferred parameter ranges in 2HDM models of Type I and Type II, the most significant changes being slight upward shifts of the central $\mu_{gg}(\gamma\gamma)$ and $\mu_{gg}(VV)$ values. In both Type I and Type II this results in the exclusion of points with too low $\mu_{gg}(\gamma\gamma)$ and/or $\mu_{gg}(VV)$. In addition, in Type II points with somewhat higher $\mu_{gg}(\gamma\gamma)$ and $\mu_{gg}(VV)$ (beyond those allowed in the 2013 analysis) are now allowed; such new points however do not occur in Type I. Apart from these small shifts the results and in particular the conclusions of [1] do not change.

A possibly important particular point is that the scenarios with low $m_A < 100$ GeV that escape all LEP and (so far) LHC limits and yet have quite substantial $gg \rightarrow A$ and bbA production cross sections survive the latest data. It will be interesting to probe these scenarios, which are possible for both Type I and Type II in the $m_h \sim 125.5$ GeV case and for Type I in the $m_H \sim 125.5$ GeV case, in ongoing analyses of the 8 TeV LHC data and in

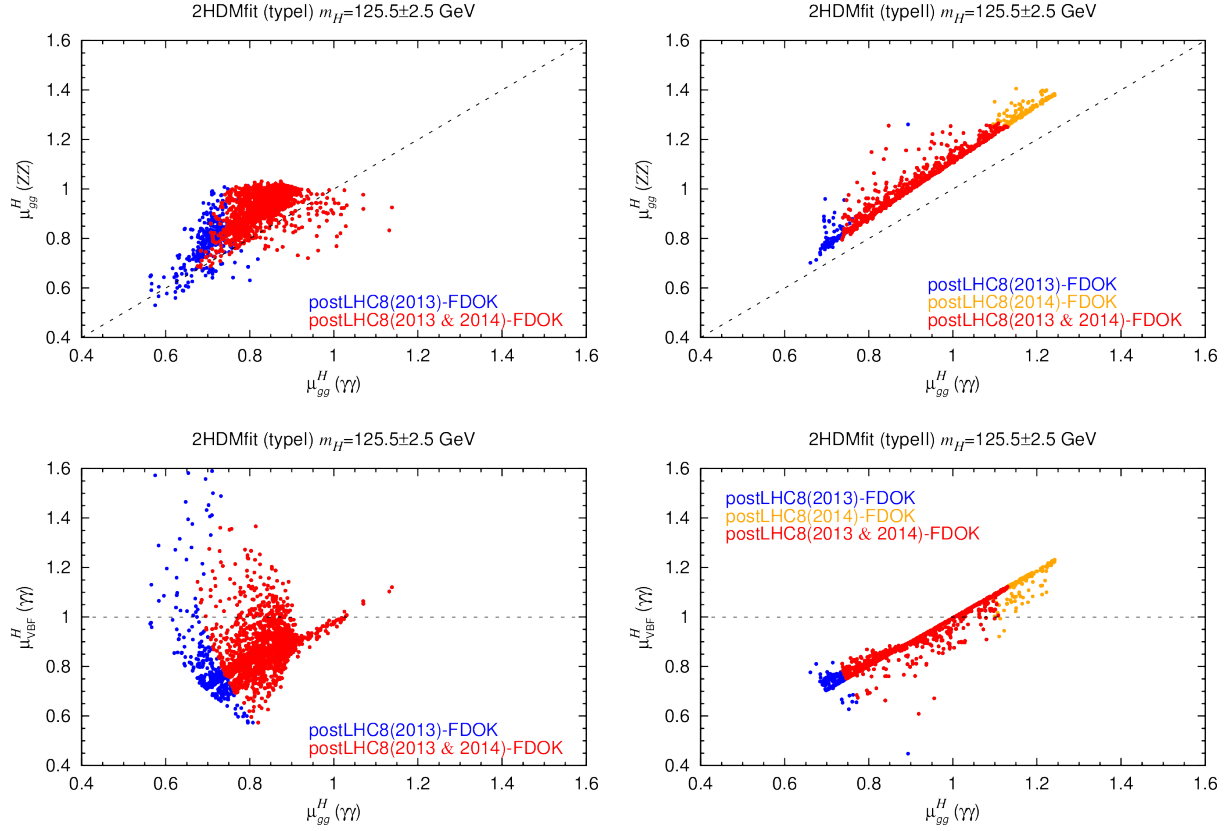


FIG. 7. Correlations of signal strengths for $m_H \sim 125.5$ GeV scenarios.

future LHC running at higher energy.

V. ACKNOWLEDGEMENTS

We thank J  r  my Bernon for discussions on the new signal strength constraints. This work was supported in part by US DOE grant DE-SC-000999 and by the “Investissements d’avenir, Labex ENIGMASS”. Y.J. is supported by LHC-TI fellowship US NSF grant PHY-0969510.

-
- [1] B. Dumont, J. F. Gunion, Y. Jiang, and S. Kraml, Phys.Rev. **D90**, 035021 (2014), arXiv:1405.3584 [hep-ph].
 - [2] G. Belanger, B. Dumont, U. Ellwanger, J. Gunion, and S. Kraml, Phys.Rev. **D88**, 075008 (2013), arXiv:1306.2941 [hep-ph].

- [3] V. Khachatryan *et al.* (CMS Collaboration), (2014), arXiv:1407.0558 [hep-ex].
- [4] G. Aad *et al.* (ATLAS Collaboration), (2014), arXiv:1408.7084 [hep-ex].
- [5] J. Bernon, B. Dumont, and S. Kraml, (2014), arXiv:1409.1588 [hep-ph].